

Preliminary Experience with Selective Laser Sintering (SLS) Models of the Human Temporal Bone

Richard A. Levy, M.D.
Department of Radiology, The University of Michigan Medical Center
1500 E. Medical Center Drive, Ann Arbor, MI 48109-0030

and
Sashidhar Guduri and Richard H. Crawford
Department of Mechanical Engineering
The University of Texas at Austin

Purpose

To assess the accuracy of three-dimensional models of the human temporal bone generated from computed tomographic (CT) data.

Materials and Methods

Thin section CT of a left human cadaveric temporal bone was performed using multiple scan planes (axial, coronal, sagittal) at 1.5 mm slice thickness, 0.25 mm pixel size with an edge enhancement 2D algorithm. CT data was converted to toggle point format based upon a threshold value of 200 obtained from prior experimentation with a CT phantom (unpublished data). Selective Laser Sintering of polycarbonate powder was performed at a beam thickness of 0.060 inches, 100 scan lines/inch, layer thickness of 0.010 inches, and layer repeat factor of 4. The polycarbonate models were then scanned in the axial, coronal and sagittal planes and compared with the original CT data. Anatomic dissection of the models was performed for further verification of the imaging findings.

Results

Models of high anatomic accuracy were generated. Shortening along the Z axis secondary to the layer repeat factor of 4 resulted in distortion of the models. No distortion in the XY plane was observed. Differences in model accuracy based upon initial CT scan plane were observed. A significant amount of non- or partially-sintered polycarbonate resulted in intermediate density on the CT images.

Conclusions

Selective Laser Sintering can result in accurate modeling of detailed anatomic structures in the human temporal bone. Further investigation of factors contributing to the accuracy of SLS in the manufacturing of high-resolution anatomic models is warranted.

References

Levy, R.A. Three-dimensional Model Generation Using Multiple Angle Tomographic Scan Planes. Patent Pending.

Levy, R.A., Edwards, W.T., Mayer, J.R. and Rosenbaum, A.E. Facial Trauma and 3-D Reconstructive Imaging: Insufficiencies and Correctives. AJNR 13:885-892, May/June 1992.

Acknowledgment

We wish to thank Mike Disher, M.D., Department of Otolaryngology, University of Michigan Hospitals, for his dissections of the anatomic models.

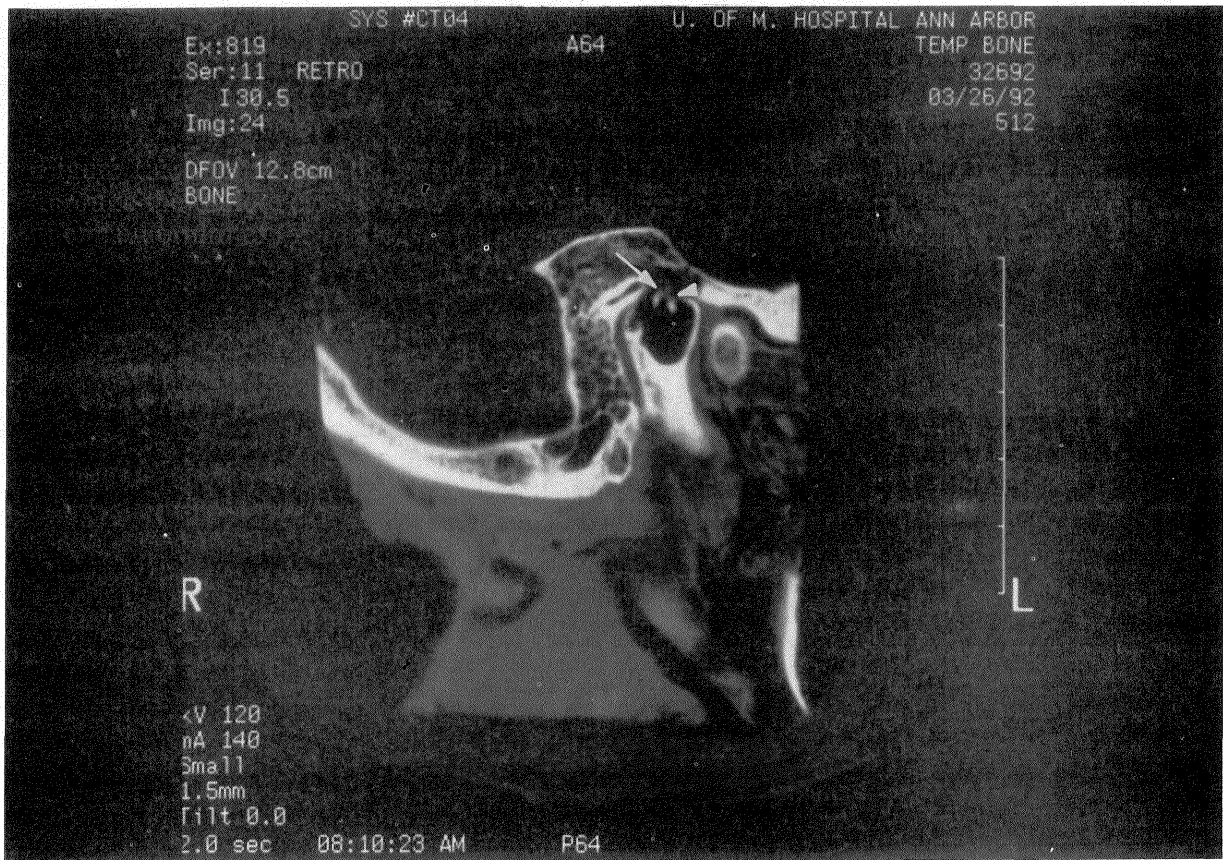


Figure 1a: Sagittal two-dimensional (2D), computerized tomographic (CT) section, through the middle ear cavity of a left human temporal bone. White arrowhead points to the manubrium of the malleus. White arrow points to the long crus of the incus.

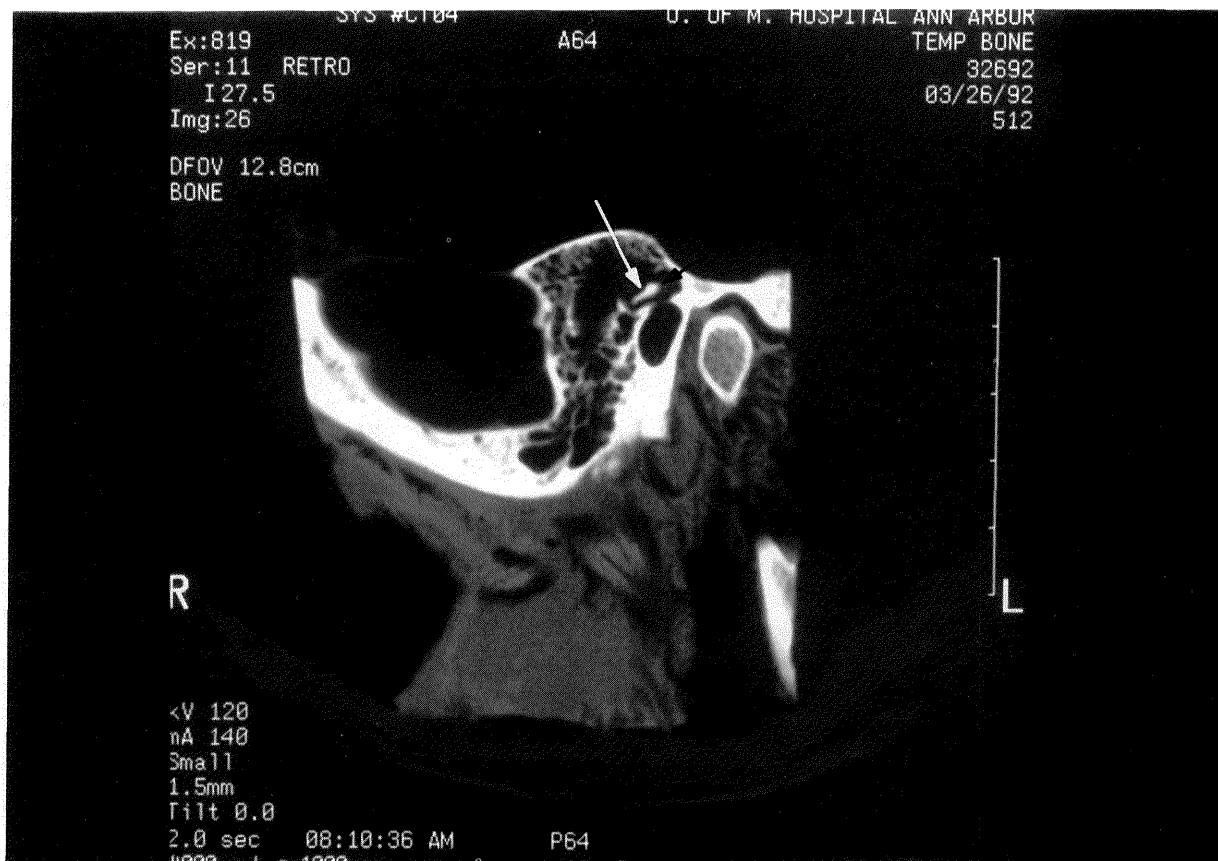


Figure 1b: Sagittal 2D CT section lateral to that in Figure 1a. White arrow points to incudomalleolar articulation. Black arrow points to head of malleus.



Figure 1c: Sagittal CT section of SLS polycarbonate model generated from sagittal data corresponding to CT image in Figure 1a. Black arrowhead points to manubrium of the malleus. Black arrow points to long crus of the incus.



Figure 1d: Sagittal CT image of model generated from sagittal CT data corresponding to image in Figure 1b. Region of incudomalleolar articulation is identified, less distinct than on the corresponding CT image in Figure 1b (black arrowhead).



Figure 1e: Post-dissection sagittal CT scan of polycarbonate model generated from sagittal CT data corresponding to imaging plane in Figure 1c. White arrow indicates "resected" area of loose polycarbonate powder in the middle ear cavity, now showing normal air density. Black arrow points to head of malleus, better appreciated than in Figures 1a and 1c, and similarly to Figure 1b.

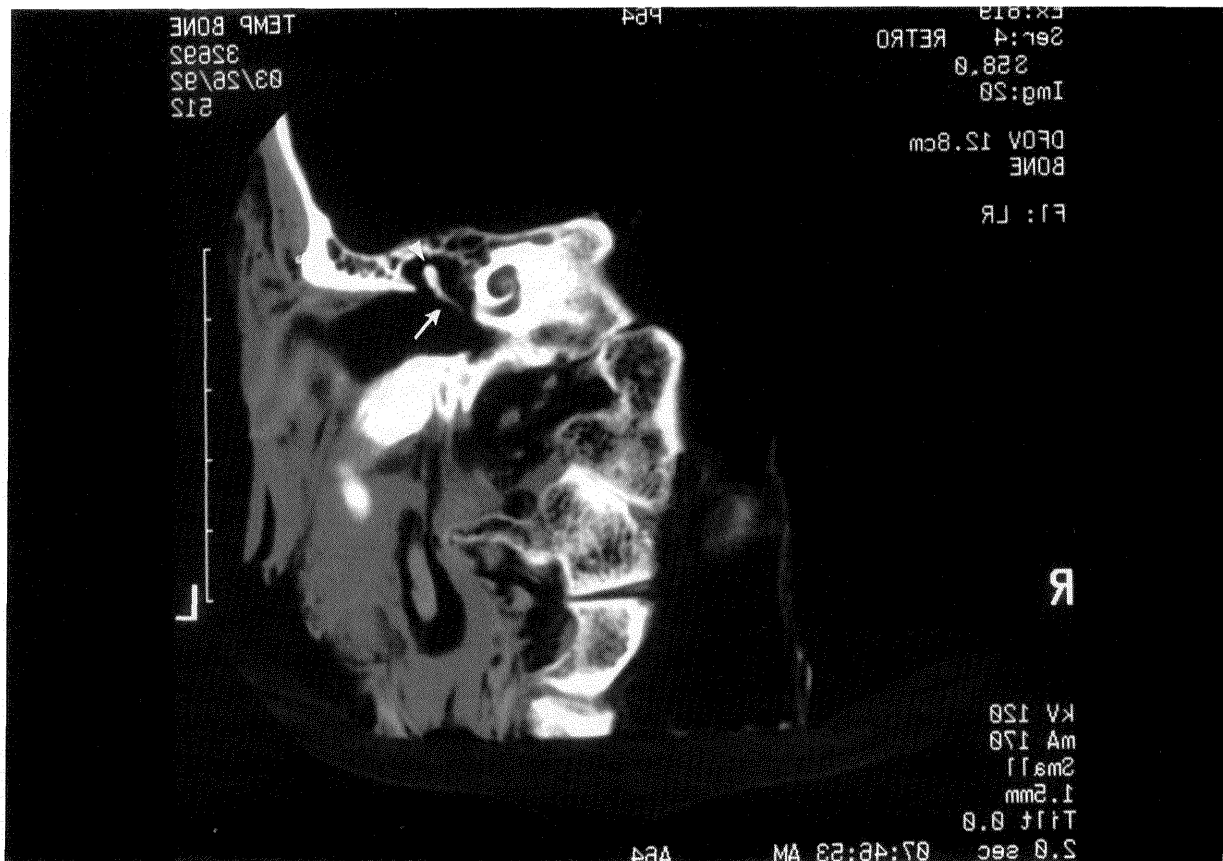


Figure 2a: Coronal 2D CT section through the same specimen as in Figure 1. Note mirror-image reversal from the polycarbonate model in Figure 2c. White arrowhead points to head of malleus. White arrow points to the manubrium of the malleus.

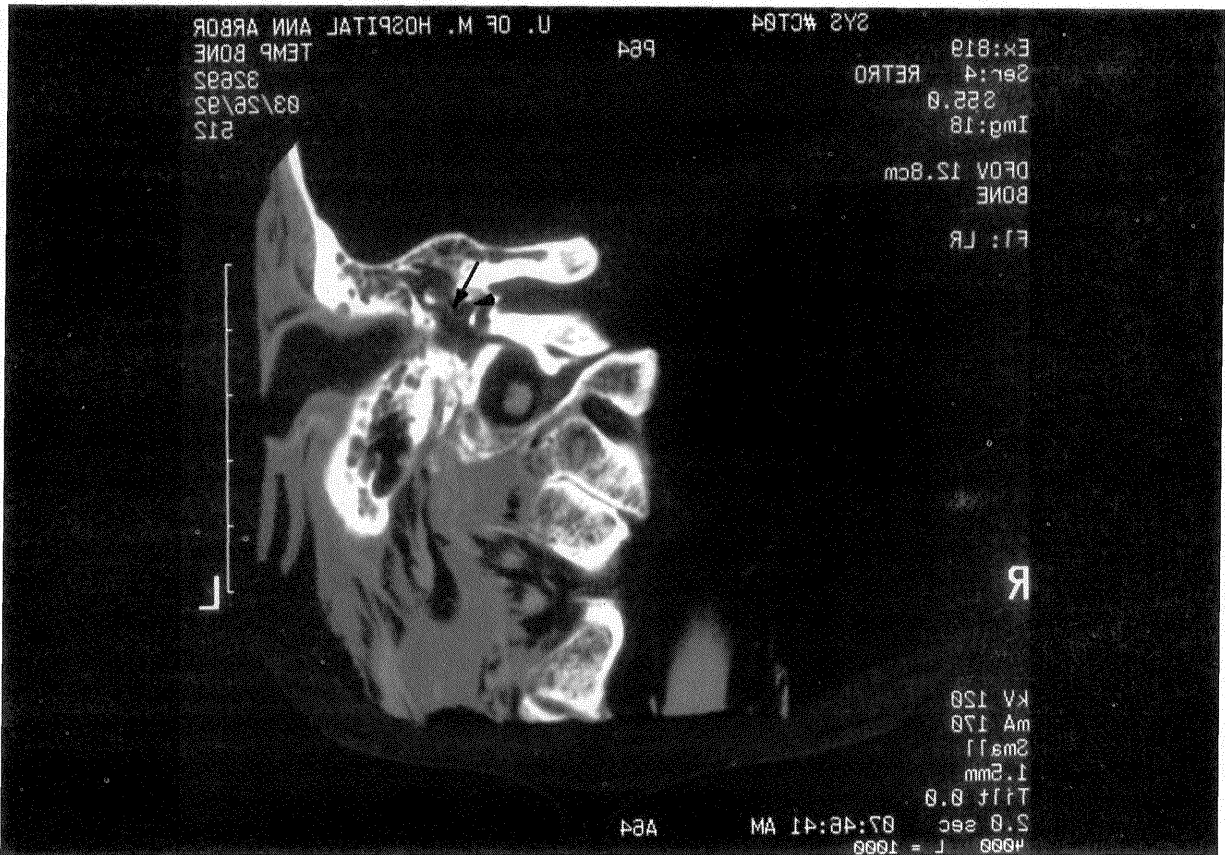


Figure 2b: Coronal 2D CT section posterior to that in Figure 2a. Black arrow points to long crus of incus. Black arrowhead points to region of oval window and stapes footplate.

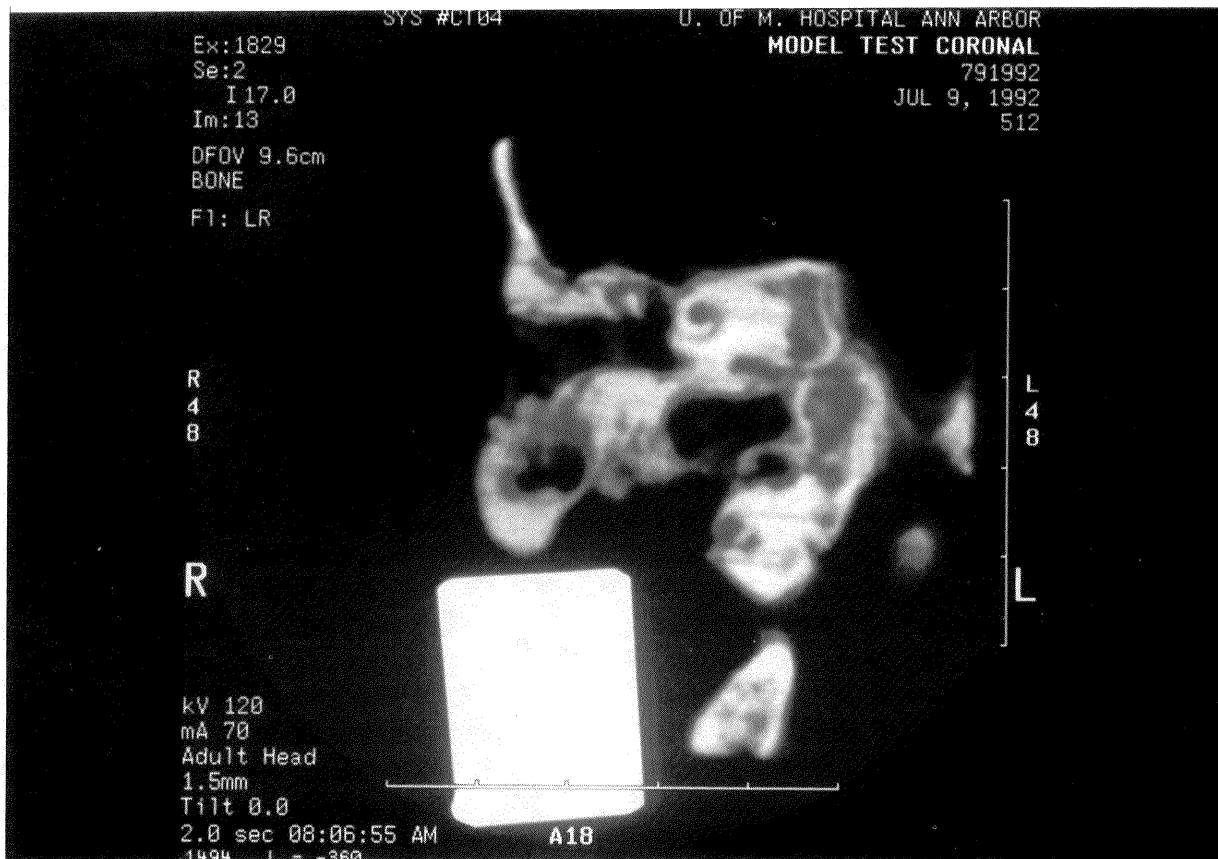
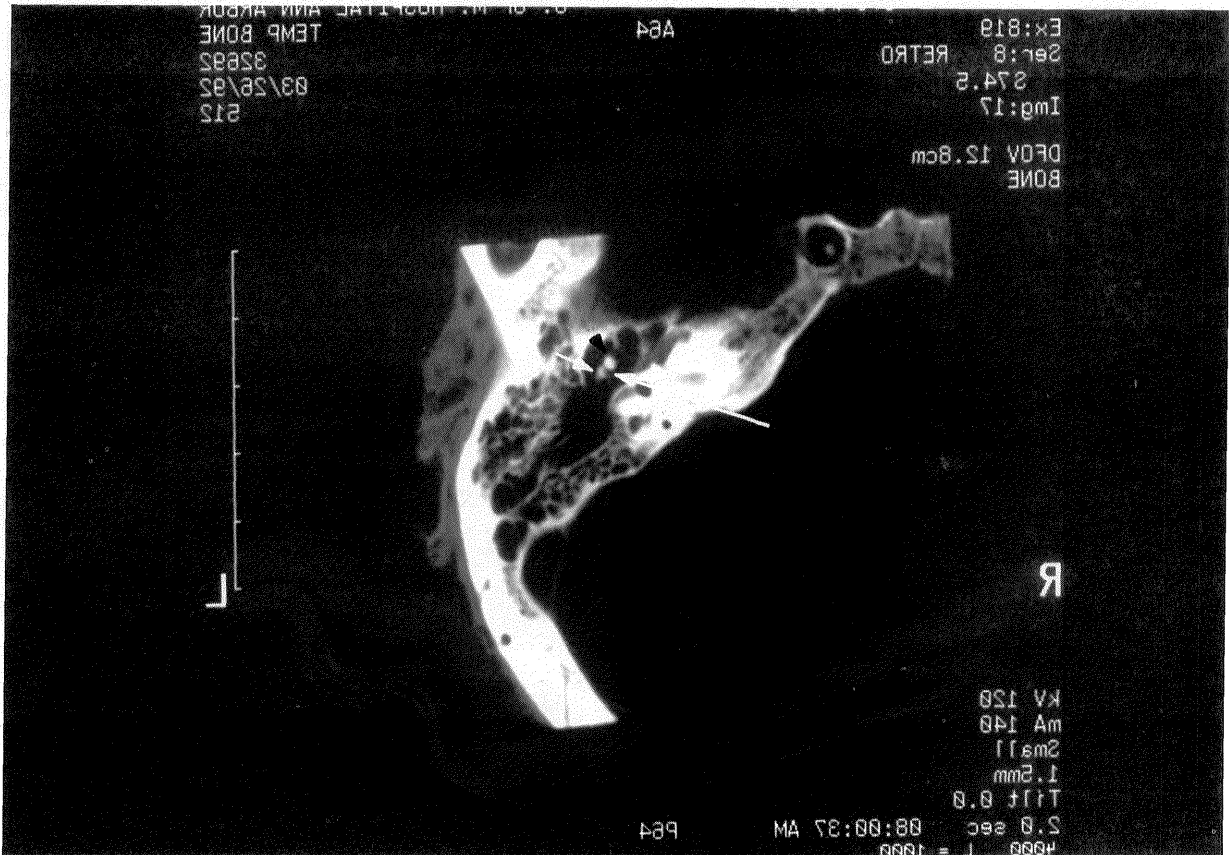


Figure 2c: Coronal CT scan of polycarbonate model generated from coronal 2D CT data. Only the head of the malleus is reproduced. The model generated from the sagittal plane (Figure 1) more accurately reproduces ossicular anatomy than does that generated from the coronal plane. This was verified at dissection.



(Figure 3a)

Figures 3a&b: Axial CT sections through the same specimen as in Figures 1 and 2. Black arrowhead points to head of malleus. Short white arrows point to body and short crus of incus. Long white arrow points to the incudomalleolar articulation. Note mirror image reversal from model in Figures 3c and d.



(Figure 3b)



(Figure 3c)

Figures 3c and d: Axial CT sections through polycarbonate models generated from axial CT data corresponding to the images in Figures 3a and b. Black arrowheads point to head of malleus. Short white arrows point to incus, as in Figures 3a and b. The manubrium of the malleus or long crus of the incus were not reproduced by SLS, although present on the initial axial CT sections (not shown).



(Figure 3d)